AASCIT **American Association for Science and Technology**

A Thermal Assessment for Vertical Helical Immersion Coil Evaporator in a Water Chiller

Ali Hussain Tarrad[1], Fouad Alwan Saleh[2], Deyaa M. Mahmood[3]

[1]Private Consultant Engineer, Mechanical Engineering, Copenhagen, Denmark
[2]Mechanical Engineering Department, College of Engineering, Al-Mustansiriya University, Baghdad, Iraq
[3]Technical Training Department, Technical Institute, the Foundation of Technical Institutes, Baghdad, Iraq

Email address

dr.alitarrad@yahoo.com (A. H. Tarrad), foads2003@yahoo.com (F. A. Saleh),
deyaa82_eng@yahoo.com (D. M. Mahmood)

Citation

Ali Hussain Tarrad, Fouad Alwan Saleh, Deyaa M. Mahmood. A Thermal Assessment for Vertical Helical Immersion Coil Evaporator in a Water Chiller. *American Journal of Energy and Power Engineering*. Vol. 2, No. 5, 2015, pp. 62-73.

Abstract

The present investigation represents a mathematical model for the steady state thermal rating of immersed coil evaporator type. A new computation method implemented the segment-by-segment technique to simulate the shell and coil heat exchanger. The evaporator helical coil is divided according to this technique into a number of small elements to be accommodated by the surrounding shell zone. Each element and its surrounding treated as a single tube heat exchanger and modeled one by one along the refrigerant flow direction. Experimental data obtained from a water chiller of the immersed coil and shell (*ICHE*) type was used for the simulation process. Four different refrigerants were used for the verification of the present model namely R22, R134a, R404A and R407C for water entering temperature range of (10-21) ºC and (400) l/hr flow rate. The model predicted the experimental values of the water chiller capacity and evaporator exit water temperature within (12%) and (4%) respectively.

1. Introduction

Heat exchangers are used in a variety of industrial applications such as air conditioning and refrigeration systems, petroleum and power plants technology, food and medicine industry and many other sectors. Engineers are looking for the most appropriate design where thermal performance and hydrodynamic measures are optimum with lowest power consumption and cost. The shell and coil heat exchanger type has been implemented for a long time due to its simple design and flexibility of operation.

Patil et al. (1982) [1] presented a procedure to the thermal design of the shell and coil heat exchangers. This design model was limited to the single-phase fluid flow only, where no change of phase to take place. There was no conclusion for the marginal error of their design procedure and its application borders. Domanski (1989) [2] developed a computer simulation program of modeling air cooled evaporator finned tube heat exchanger for air conditioning system. The model based on tube-by-tube approach in forward iteration scheme. The percentage of discrepancy between the experimental and predicted total cooling capacity was (-6 %).

Avina (1994) [3] developed a model for a shell and coil single phase heat exchanger used in solar domestic hot water system. The model based on the effectiveness *NTU*

method, with a combined heat transfer mode; natural and forced convection; to determine the heat transfer coefficient over the tubes. The heat exchanger was treated as one section. The helical coil geometry was modified to a bundle of tubes in cross flow, each turn assumed to be a straight tube. Naphon (2007) [4] investigated the thermal performance and pressure drop of two types of helical coils, smooth and enhanced surfaces, immersed in a shell heat exchanger. The helical coil was made of 9.5 mm copper tube, where cold and hot water were circulated through the shell and coil side respectively with good range of flow rate and temperature.

Amitkumar Andhare (2015) [5] focused on the design of a horizontal shell and helical coil heat exchanger and its thermal evaluation with counter flow configuration. The thermal analysis was carried out considering the various parameters such as flow rate of cold water, flow rate of hot water, temperature, effectiveness and overall heat transfer coefficient. They concluded that the design procedure adopted gives sizing and rating analysis of helical coil heat exchanger and results were found in good agreement with the experimental results.

The present work is focused on the thermal and hydrodynamic aspects of the vertical shell and coil evaporator type. Experimental data were obtained from a water chiller designed to be capable to handle a variety of refrigeration capacity. Entering water temperature was controlled in the range of (10- 21) °C at water flow rate of (400) l/hr. A model for the rating prediction of the coil and shell evaporator was built to study the drop-in technique of three refrigerant alternatives for the R22 one. Table (1) shows selected properties for the refrigerants implemented in the present model verification, Mahmood (2010) [6].

2. Experimental Category

2.1. General Description

The used experimental rig is comprised of a water chiller which was built for the objective of the present work. It circulates R-22 as a refrigerant having a cooling capacity of (1.5 kW). The apparatus arrangement together with the instrumentation and measurement devices are shown in figure (1). It consists of the basic components required for the refrigeration cycle namely, evaporator, condenser, compressor and expansion device. The refrigerant side flow arrangement and instrumentation are installed at selected ports around the rig on both of the refrigerant and water sides. The water path

through the chiller is shown schematically in figure (2) for which the temperature and flow rate were measured at the entering and leaving sides.
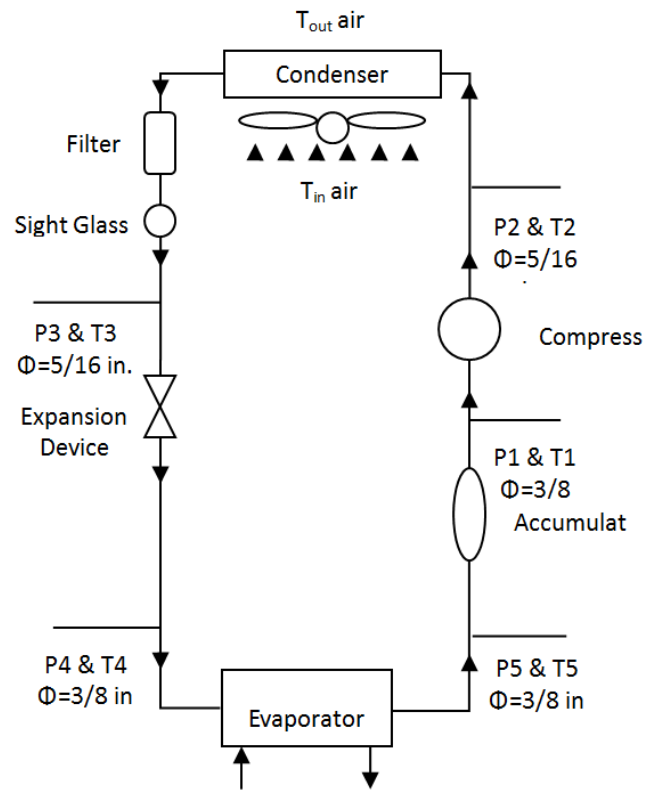

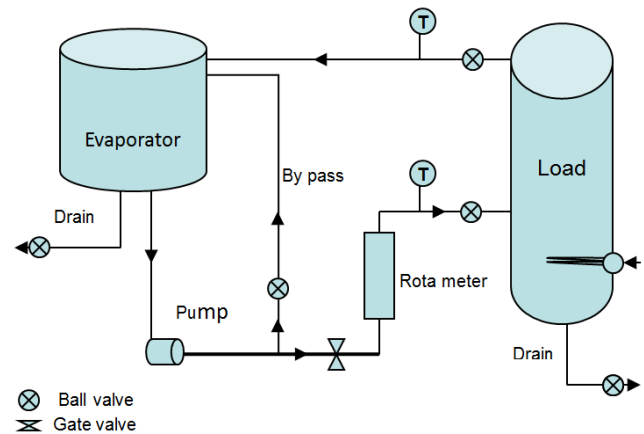**Figure (1).** A schematic diagram for the refrigerant side of the chiller, Mahmood [6].

Figure (2). A schematic diagram for the water side path of the test unit, Mahmood [6].

Table (1). Selected thermal properties of studied refrigerants, Mahmood [6].

Properties	R-22	R-134 a	R-407C	R-404A
Molecular Weight	86.47	102.03	86.2	97.6
Boling Temperature* (°C)	-40.81	−26.06	-43.8	-46.6
Critical Temperature (°C)	96.15	101.08	86.4	72.1
Critical Pressure (Bar)	49.9	40.6	46.3	37.4
Temperature Glide (K)	0	0	7.1	0.8
Ozone Depletion Potential (ODP)	0.034	~ 0	~ 0	~ 0
Global Worming Potential (GWP)	1780	1320	1700	3750

Properties	R-22	R-134 a	R-407C	R-404A
Lifetime (τ)	12.0	14.0	a	a
Thermodynamic Property @	8 (°C)	8 (°C)	8 (°C)	8 (°C)
Latent Heat (kJ/kg)	198.42	192.47	201.78	158.4
Saturated Vapor Specific Volume (kg/m³)	0.0368	0.0528	0.0389	0.0255
Saturated Liquid Density (kg/m³)	1254	1267	1206	1119
Saturated Vapor Specific Heat (kJ/kg.K)	0.775	0.920	1.0054	1.0567
Saturated Liquid Specific Heat (kJ/kg.K)	1.193	1.360	1.4470	1.4269
Thermodynamic Property @	48 (°C)	48 (°C)	48 (°C)	48 (°C)
Latent Heat (kJ/kg)	156.8	154.39	152.12	107.12
Saturated Vapor Specific Volume (kg/m³)	0.01226	0.01598	0.0116	0.0077
Saturated Liquid Density (kg/m³)	1092	1111	1025	913
Saturated Vapor Specific Heat (kJ/kg.K)	1.0857	1.196	1.4366	1.7562
Saturated Liquid Specific Heat (kJ/kg.K)	1.4007	1.553	1.7549	1.8976

* at one atmospheric pressure.

a. atmospheric lifetime are not given for blend since the components separate in the atmosphere

A water centrifugal pump is used to circulate water between the evaporator vessel and external load. The flow rate of the pump is (5-30) l/min with a head of (5.5-28) m. The external load is represented by an (85) liter water tank capacity equipped with electrical heater of (2000) watt. It is made of insulated steel cylindrical vessel of (40) cm diameter and (68) cm height. The water piping system was provided with a bypass loop for the control purpose of the chiller capacity and cycling mode tests.

2.2. Evaporator

A shell and coil evaporator was designed and fabricated in the local market workshops, figure (3). The physical characteristic and dimensions of the evaporator mechanical design are listed in table (2). The immersion coil is made of a copper (9.52 mm) outside diameter tube having (15 m) length consisting of (20) turns. The refrigerant flows inside the copper

helical coil, whereas the water is circulated on the shell side.

Table (2). *Evaporator physical dimensions and characteristics, Mahmood [6].*

Dimension specification	Evaporator
Shell diameter (mm)	300
Shell height (mm)	300
Shell volume (liter)	20
Shell material	Stainless steel
Thermal conductivity of shell metal (W/m.K)	15
Coil mean diameter (mm)	250
Coil tube length (m)	15
Number of coils turns	20
Inside tube diameter (mm)	7.93
Outside tube diameter (mm)	9.52
External coil surface area (m2)	0.448
Tube material	Copper
Thermal conductivity of tube (W/m.K)	401

(a) Shell of evaporator

(b) Coil of evaporator
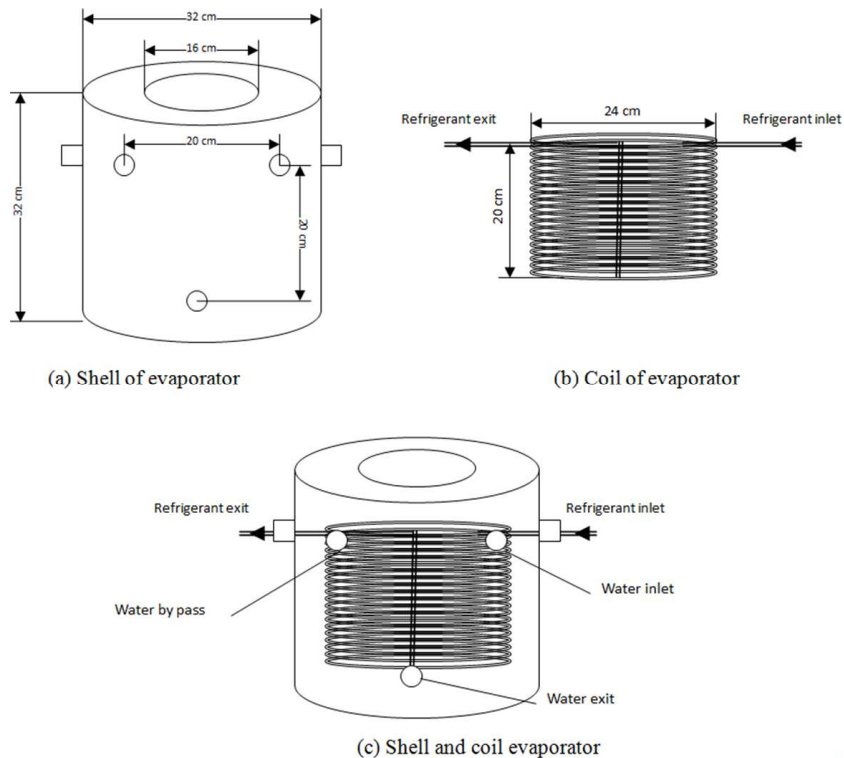
(c) Shell and coil evaporator

Figure (3). *A schematic diagram of the shell and coil evaporator, Mahmood [6].*

The test condenser is an air cooled finned tube heat exchanger. It consists of three rows each with (10) copper tubes having (9.52) mm outside diameter and (254) mm length with aluminum fins. A reciprocating hermetic compressor charged with polyolester oil as a lubricant. This type of oil is suitable to be used with HCFC such as R22 refrigerant and working with the test HFC refrigerant. The expansion device was (90) cm copper capillary tube of (1) mm internal diameter and external diameter of (2) mm. It was selected and installed as a part of the experimental test rig according to ASHRAE (1979) [7]. The evaporator shell, water pump and piping system were completely insulated with a sheet of Armaflex having a thickness of (25) mm and thermal conductivity of (k = 0.036 W/ m.K). Full details for the experimental rig set-up and construction may be found in Mahmood [6].

3. Modeling Methodology

The evaporator is a helical coil immersed in a vertical stainless steel cylindrical shell, figure (3). The refrigerant flows inside the tube coil, while the water flows on the shell side over the tubes. The idea of the model is withdrawn from the fact that each coil turn represents an independent heat exchanger. Following the work of Tarrad and coworkers; [8], [9] and [10] a new computation method was based on segment-by-segment technique used to simulate the shell and coil evaporator. The evaporator helical coil is divided according to this technique into turns and consequently the turn was subdivided into small increments. Each element is treated as a single tube heat exchanger and is modeled one by one along the refrigerant flow direction.

The major evaporator model assumptions are:

- The water mass flow rate is assumed to be uniformly distributed over the whole length of evaporator coil turn on the shell side.
- A perfect cross flow heat exchanger was considered for each segment and turn. Hence, the water temperature inlet to the evaporator coil turn assumed to be the same for each element of the turn.
- The step by step technique states that the average water exit temperature of each turn is considered to be the inlet to the next turn.
- The segment of the evaporator coil turn having a length of (75 mm) is considered as straight tube.
- The refrigerant side outlet operating conditions such as temperature, pressure and vapor quality were considered to be as the inlet for the next segment of the turn and so on.
- The enhanced heat transfer due to the swirling motion of water over the helical evaporator coil was neglected.

It is worth mentioning that Mahmood [6] stated that the experimental data has a certainty for the measured performance parameters to fall within (± 2%). The most attractive feature of the present model is the implementation of the simple available correlations for the heat transfer rate and pressure drop in the open literature.

3.1. Basic Equations

Figure 4 shows the control volume of a tube element and reveals the inlet and outlet parameter for the tube calculations. A detailed derivative for these equations is presented by Tarrad [12] for flow inside tubes.
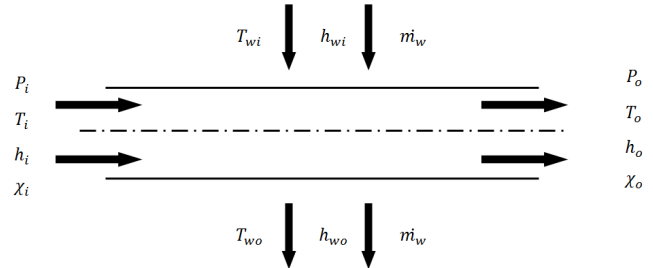

Figure (4). *Control volume of an individual tube segment, Tarrad and Al-Nadawi (2010) [11].*

For steady flow process through the heat exchangers, the conversation of mass principle of control volume can be expressed as:

$$\sum_{in} \dot{m} = \sum_{out} \dot{m} \qquad (1)$$

The energy equation for a fixed control volume can be expressed by:

$$\dot{Q}_{net,in} = \sum_{out} \dot{m} h - \sum_{in} \dot{m} h \qquad (2)$$

These expressions for the mass conservation and energy balance, (1) and (2) respectively were implemented in the present rating model.

3.2. Refrigerant Side Heat Transfer Coefficient

3.2.1. Single Phase Flow Heat Transfer Coefficient

The single phase forced convection heat transfer coefficient for a superheated region, turbulent flow, heated tube is calculated by using Dittus-Boelter correlation, Incropera and DeWitt (1996) [13] as the following:

$$\alpha_g = 0.023 \, Re_g^{0.8} \, Pr_g^{0.4} \left(\frac{k_g}{d_i} \right) \qquad (3)$$

3.2.2. Two Phase Flow Heat Transfer Coefficient

Refrigerant flow with evaporation is subdivided in the model in two flow patterns; annular flow and mist flow. The quality value of (0.85) was selected in the model as the border point between these two flow patterns, Domanski (1989) [2].

(i). Annular Flow Heat Transfer Coefficient

The correlation developed by Gungor and Winterton (1986) [14] was used to evaluate the evaporative heat transfer coefficient for R-22. The form of the correlation is consistent with Chen approach (1966) [15] in that, it recognizes two

distinct mechanisms for the heat transfer; nucleate boiling and forced convection. Their correlation has a high certainty and well tested for R22 and has the form:

$$\alpha_{tp} = E\,\alpha_l + S\,\alpha_{nb} \tag{4}$$

Where (α_l) liquid convection heat transfer coefficient calculated by using Dittus-Boelter correlation for the turbulent flow, Incropera and DeWitt (1996) [13] as the following:

$$\alpha_l = 0.023\,Re_l^{0.8}\,Pr_l^{0.4}\left(\frac{k_l}{d_i}\right) \tag{5}$$

In which the liquid Reynolds (Re_l) based on fraction of liquid mass flux is estimated as:

$$Re_l = \frac{G\,(1-x)d_i}{\mu_l} \tag{6}$$

While the liquid Prandtl (Pr_l) is:

$$Pr_l = \frac{\mu_l\,cp_l}{k_l} \tag{7}$$

The nucleate pool boiling coefficient (α_{nb}) is obtained with Cooper (1984) [16] equation:

$$\alpha_{nb} = 55\,p_r^{0.12}\,(-0.4343\,\ln p_r)^{-0.55}\,M^{-0.5}\,q^{0.67} \tag{8}$$

The two phase convection multiplier (E) is a function of the Martinelli parameter and also the heat flux via the Boiling number:

$$E = 1 + 24000\,Bo^{1.16} + 1.37\left(\frac{1}{X_{tt}}\right)^{0.86} \tag{9}$$

The boiling number (Bo) defined as:

$$Bo = \frac{q}{G\,h_{fg}} \tag{10}$$

It represents the ratio of the actual heat flux to the maximum heat flux achievable by complete evaporation of the liquid. The Martinelli parameter (X_{tt}) is defined as:

$$X_{tt} = \left(\frac{1-x}{x}\right)^{0.9}\left(\frac{\rho_g}{\rho_l}\right)^{0.5}\left(\frac{\mu_l}{\mu_g}\right)^{0.1} \tag{11}$$

The boiling suppression factor (S) is estimated by:

$$S = \left\{1 + 0.00000115\,E^2\,Re_l^{1.17}\right\}^{-1} \tag{12.a}$$

In the case of a horizontal tube, if the Froude number (Fr), was smaller than (0.05), then (E) and (S) should be multiplied by (E_2) and (S_2) respectively:

$$E_2 = Fr_l^{(0.1-2\,Fr_l)} \tag{12.b}$$

$$S_2 = Fr_l^{0.5} \tag{12.c}$$

While the liquid Froude number is defined as:

$$Fr = \frac{G^2}{\rho_l^2\,g\,d_i} \tag{12.d}$$

A new version of Gungor and Winterton (1987) [17]

correlation was used to calculate the evaporative heat transfer coefficient for R-134a as recommended by Thome (1997) [18]. This correlation was based only on convective boiling:

$$\alpha_{tp} = E_m\,\alpha_l \tag{13.a}$$

Their new two phase convective multiplier E_m is:

$$E_m = 1 + 3000\,Bo^{0.86} + 1.12\left(\frac{x}{1-x}\right)^{0.75}\left(\frac{\rho_l}{\rho_g}\right)^{0.41} \tag{13.b}$$

(α_l) is calculated by using Dittus-Boelter correlation based on the local liquid fraction of the flow.

Bivens and Yokozeki (1994) [19] correlation was used to evaluate the evaporation heat transfer coefficient of mixture refrigerants, R-407C and R-404A. This correlation took into account the effect of mass transfer resistance developed in boiling mixtures.

$$\alpha_{tp,mixture} = \frac{\alpha_{tp}}{\left(1 + \frac{\alpha_{tp}\,T_{int}}{q}\right)} \tag{14.a}$$

Where T_{int} is the temperature at the liquid-vapor interface estimated as:

$$T_{int} = 0.175\,(T_d - T_b)\left[1 - \exp\left(\frac{q}{1.3\times10^{-4}\,\rho_l\,h_{fg}}\right)\right] \tag{14.b}$$

The two phase heat transfer coefficient is presented as:

$$\alpha_{tp} = (\alpha_{nb}^{2.5} + \alpha_{bc}^{2.5})^{1/2.5} \tag{14.c}$$

The convection heat transfer coefficient defined as:

$$\alpha_{bc} = F\,\alpha_l\,R \tag{14.d}$$

and

$$F = \left(0.29 + \frac{1}{X_{tt}}\right)^{0.85} \tag{14.e}$$

Here (F) is a function of Martinelli parameter (X_{tt}) defined early.

If $Fr_l \leq 0.25$, $R = 2.838\,Fr_l^{0.2}$
If $Fr_l > 0.25$, $R = 2.15$

(ii). Mist Flow Heat Transfer Coefficient

The heat transfer coefficient for the mist flow (α) for flow quality range from (0.85) to (1), is calculated according to Domanski (1989) [2]:

$$\alpha = \frac{(1-x)\,\alpha_{tp} + (x-0.85)\,\alpha_g}{0.15} \tag{15}$$

Where α_{tp} is calculated from the proper expression for the pure and blend refrigerants.

3.3. Water Side Heat Transfer Coefficient

The heat transfer coefficient of water consists of combined effect of free and forced convection heat transfer mode according to the parameter (Gr/Re^2). Natural convection is negligible when (Gr/Re^2) < 0.1, forced convection is negligible when (Gr/Re^2) > 10, and neither of them is negligible when 0.1

$< (Gr/Re^2) < 10$. In the present work, the parameter (Gr/Re^2) was within the latter range. Therefore, both of heat transfer modes (natural and forced) were considered. A review of experimental data suggests a correlation of the form:

$$Nu_{comb} = \left(Nu_f{}^n \mp Nu_n{}^n\right)^{1/n} \quad (16)$$

Where Nu_f and Nu_n are determined from the correlations for pure forced and natural (free) convection respectively. The plus sign is for assisting and transverse flows, and the minus sign is for opposing flows. The best correlation of data is generally obtained for (n=3), the present work used (n=4) as stated in Incropera and DeWitt (1996) [13] for cylindrical geometry.

3.3.1. Forced Convection Heat Transfer Coefficient

The forced convection heat transfer coefficient of water is calculated by using the general correlation, Cengel (1998) [20]:

$$Nu_f = c\,Re_d{}^m\,Pr^n \quad (17)$$

Where the (n=1/3) and the experimentally determined constants, (c) and (m) are given in table (3).

Table (3). Constants for use with equation (17).

Re	c	m
0.4-4	0.989	0.330
4-40	0.911	0.385
40-4000	0.683	0.466
4000-40000	0.193	0.618
40000-400000	0.0266	0.805

3.3.2. Free Convection Heat Transfer Coefficient

Churchill and Chu (1975) [21] correlation was used to calculate Nusselt numbers of free convection between evaporator tubes and water, it is suitable for wide range of Ra $(10^{-5} < Ra < 10^{12})$:

$$Nu = \left\{ 0.6 + \frac{0.387\,Ra^{1/6}}{\left[1 + \left(\frac{0.559}{Pr}\right)^{9/16}\right]^{\frac{8}{27}}} \right\}^2 \quad (18.a)$$

Where (Ra) is Rayleigh numbers defined as:

$$Ra = Gr\,Pr \quad (18.b)$$

And (Gr) is Grashof numbers defined as:

$$Gr = \frac{g\,\beta\,(T_s - T_\infty)\,d_o{}^3}{\nu^2} \quad (18.c)$$

All thermal properties were calculated at the film temperature according to Holman (2002) [22].

$$T_f = \frac{T_s + T_\infty}{2} \quad (18.d)$$

The surface temperature was assumed to be the refrigerant side temperature which was close to the inner surface of the coil due to the high thermal conductivity of the tube.

3.4. NTU Effectiveness Relations

For any heat exchanger, the total heat rejected from the hot fluid is dependent on the heat exchanger effectiveness and the heat capacity of each fluid.

$$Q = \varepsilon\,C_{min}\left(T_{h,i} - T_{c,i}\right) \quad (19.a)$$

The heat capacity, C, the extensive equivalent of the specific heat, determines the amount of heat a substance absorbs or rejects per unit temperature change.

$$C = \dot{m}\,cp \quad (19.b)$$

The effectiveness is the ratio of the actual amount of heat transferred to the maximum possible amount of heat transferred.

$$\varepsilon = \frac{Q}{Q_{max}} \quad (19.c)$$

For a cross-flow heat exchanger with one stream is mixed (C_{max}) and the other stream is unmixed (C_{min}), the effectiveness can be related to the number of transfer units (NTU) with the following equation, McQuiston(1994) [23]:

$$\varepsilon = \left(\frac{1}{C_r}\right)\left\{1 - exp\left[-\,C_r\left(1 - exp(-NTU)\right)\right]\right\} \quad (20.a)$$

Where

$$C_r = \frac{C_{min}}{C_{max}} \quad (20.b)$$

In the saturated portion of the evaporator, the heat capacity on the refrigerant side approaches infinity and the heat capacity ratio goes to zero. When $C_r=0$, the effectiveness for any heat exchanger configuration is:

$$\varepsilon = 1 - exp(-NTU) \quad (21)$$

The *NTU* is a function of the overall heat transfer coefficient.

$$NTU = \frac{UA}{C_{min}} \quad (22)$$

Even though the convective heat transfer coefficients may be different on the water and refrigerant sides of the heat exchanger, the UA product is the same on either side. This is because all of the heat taken from the water must be transferred to the refrigerant.

$$\frac{1}{UA} = \frac{1}{\eta_{s,w}\,\alpha_w\,A_w} + \frac{R_{f,w}}{\eta_{s,w}\,A_w} + R_w + \frac{R_{f,r}}{\eta_{s,r}\,A_r} + \frac{1}{\eta_{s,r}\,\alpha_r\,A_r} \quad (23)$$

There are no fins on the both water and refrigerant sides of the evaporator tubes; therefore, the surface efficiency for both sides is (1). The fouling factors ($R_{f,w}$) and ($R_{f,r}$) for the water and refrigerant sides are negligible. The overall heat transfer coefficient reduces to:

$$UA = \left(\frac{1}{\eta_{s,w}\,\alpha_w\,A_w} + R_w + \frac{1}{\alpha_r\,A_r} \right)^{-1} \qquad (24)$$

4. Discussion

4.1. Model Validation

The validation of the present model can be achieved by using a set of experimental data produced by Mahmood [6]. Appendix (A) represents typical set of data obtained when the suggested refrigerants were circulated throughout the water chiller on the drop-in technique.

Figure (5) shows the comparison of experimental and predicted evaporator load for R-22, R-134a, R-407C and R-404A. The maximum discrepancy percentage between experimental and predicated evaporator load was about (-12%). The estimated results by the present model for R-134a showed a better agreement with experimental data, the simulated evaporator capacity was under predicted by about (5%). The evaporator capacity of R-404A was over predicted by (4%).

Figure (6) illustrates the comparison of measured and predicted evaporator water exit temperature (EWET) for R-22, R-134a, R-407C and R-404A. The discrepancy percentage between measured and predicated (EWET) by the model varied between (0 to 4%). The simulated (EWET) of R-407C was over predicted by (4%). R-134a and R-404A showed excellent agreement between the predicted and the measured (EWET).
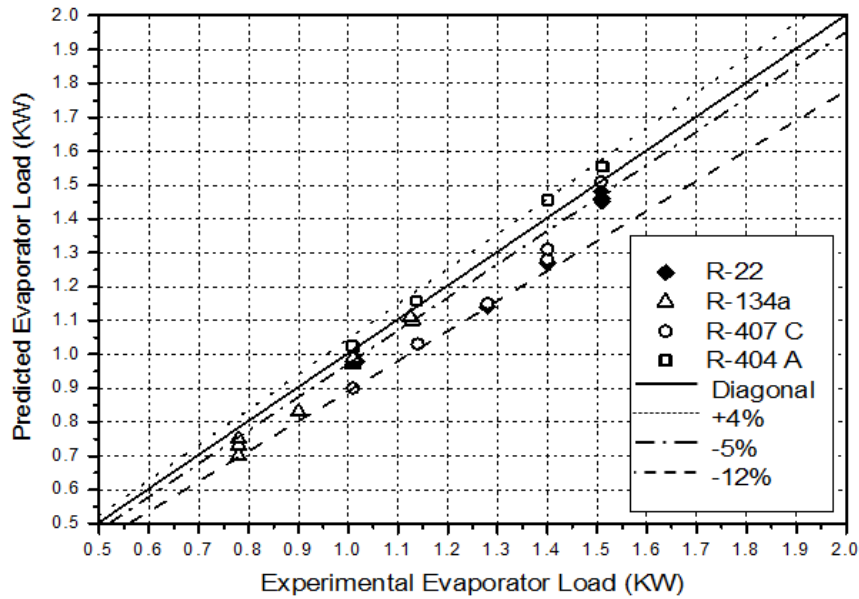

Figure (5). *Comparison of the experimental and predicted evaporator load.*
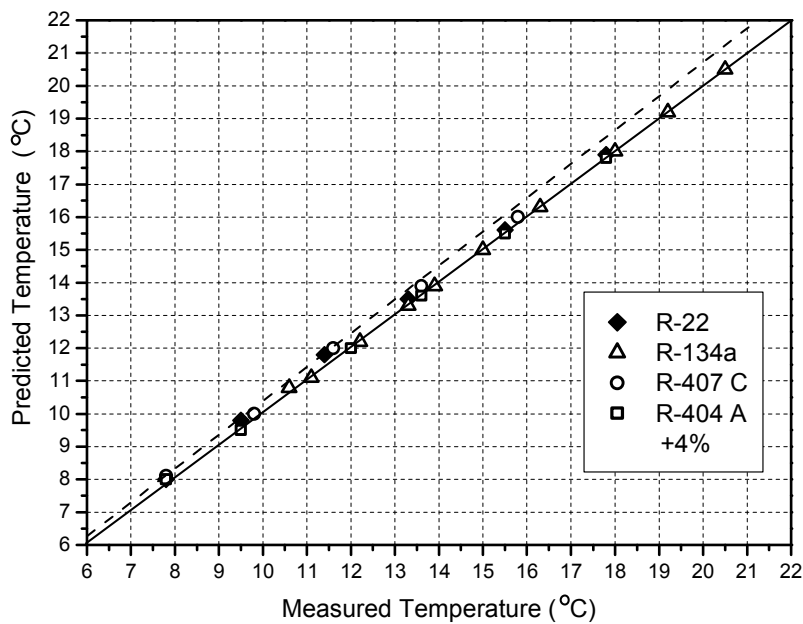

Figure (6). Comparison of the measured and predicted evaporator water exit temperature.

4.2. Refrigerant Side Heat Transfer Coefficient

Figure (7) represents the predicted refrigerant side heat transfer coefficient (RSHTC) distribution along the evaporator coil path for R-22, R-134a, R-407C and R-404A for water entering temperature of (21) °C. The refrigerant side consists of two zones; a two phase (evaporation) and a single phase (superheated). The two phase flow is subdivided into two regimes, annular flow for vapor quality (x) less than 0.85 and mist flow for (x) ranged between (0.85 and 1).
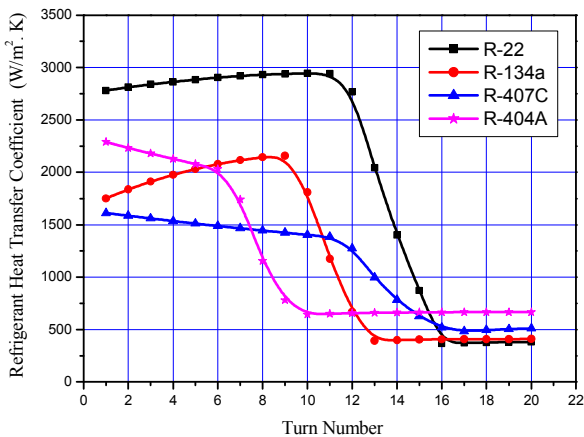

Figure (7). *Variation of local refrigerant side heat transfer coefficient with turn number.*

The pure refrigerant R-22 and R-134a, showed a slight increase in the (RSHTC) as the vapor quality is increased up to (0.85) for annular flow regimes. This is mainly due to the increase of the evaporation heat transfer coefficient which is a reflection of its predominance on the heat transfer rate. Then it was decreased sharply for mist flow down to that value corresponding to a single phase superheated vapor. In the superheated vapor, the (RSHTC) was almost constant. The mixture refrigerants R-407C and R-404A showed a slight decrease in the (RSHTC) as the vapor quality increased for the annular flow regimes of the vapor quality less than (0.85).

The two phase refrigerant heat transfer coefficient resulted of contribution of two heat transfer modes, convection heat transfer coefficient and nucleate pool boiling heat transfer coefficient. The trend of two phase heat transfer coefficient depends on the mutual effect of heat transfer modes and that could be dominant. The nucleate pool boiling decreased as the vapor quality increased due to the reduction in the heat flux, while the contribution of forced convection heat transfer coefficient was increased.

R-22 has the highest two phase refrigerant heat transfer coefficient among the tested refrigerants, it is ranged between (2780 – 2941) W/m^2.°C. The (RSHTC) of R-134a was ranged between (1751 – 2157) W/m^2.°C. This is partly because of the mass flux of R-134a, it was (151) kg/m^2.s, whereas it was (206) kg/m^2.s for R22. The (RSHTC) of R-407C which was ranged between (1384-1612) W/m^2.°C, was lower than that of R-22,

although the mass flux of R-407C is close to that of R-22. This is mainly due to the effect of mass transfer resistance. The R404A exhibited a closer heat transfer coefficient to R22 than the other refrigerants. The (RSHTC) was ranged between (2031-2288) W/m^2.°C, although the refrigerant mass flow rate was (284 kg/m^2.s) which was greater than that of R-22. In general, the boiling heat transfer coefficient of mixtures are usually less than those of pure liquids composing these mixtures due to the presence of mass transfer resistance in addition to the heat transfer resistance, Tarrad [24] (1991).

4.3. Vapor Quality Variation

The predicted vapor quality on the refrigerant side is illustrated in figure (8). It is obvious that all of the refrigerants are having the same behavior of variation for the vapor quality with the flow progress inside the coil. The model prediction showed that R-22 and R-407C exhibited almost the same vapor quality with turn number of the coil. The vaporization zone to attain saturated vapor with quality of (100%) occupies about (80%) of the total coil length. The rest of the coil length serves for the superheating purposes. The refrigerant R-404A showed the lower coil length required for the attainment of saturated vapor, it occupies about (50%) of the total coil length. This measure is reflected on the total coil load as will be described later. R-134a showed a vapor saturated length of (65%) of the total coil length.
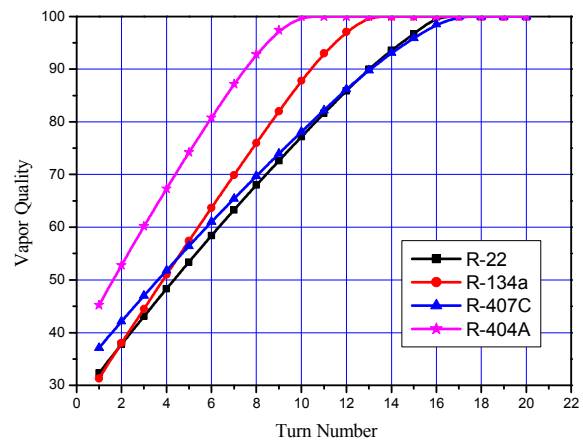
Figure (8). *Variation of local refrigerant side vapor quality with turn number.*

4.4. Total Evaporator Coil Load

Figure (9) illustrates the predicted total evaporator coil refrigeration load variation with number of turns of R-22, R-134a, R-407C and R-404A. The tested refrigerants exhibited similar behavior, the heat gain increased gradually in linear relation for the two-phase zone. After that through the superheated zone, the evaporator coil revealed a very slight increase in heat gain which is almost constant. It is clear that the heat transfer rate during superheated zone is low due to the reduction in the heat transfer coefficient and temperature difference.
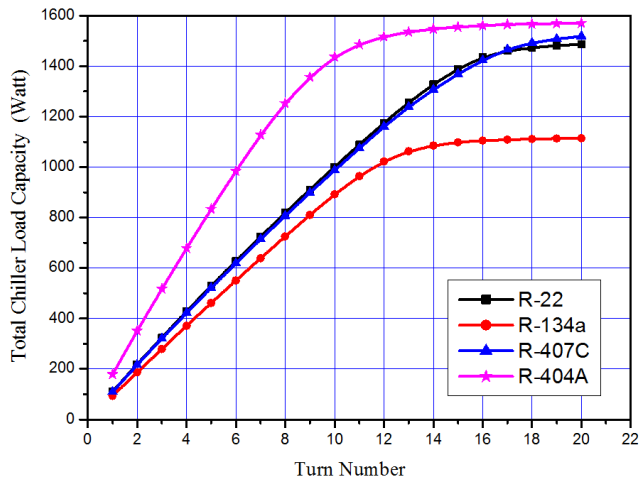
Figure (9). The total evaporator coil refrigeration load variation with number of turn.

The total predicted evaporator refrigeration load of the simulated refrigerants are (1485 W), (1114 W), (1517 W) and (1570 W) for R-22, R-134a, R-407C and R-404A. It is obvious that the evaporator load when circulating R-134a is the lowest; this is partly due to its lower mass flux (G), and consequently lower heat transfer coefficient. The evaporator load of R-404A was close to those of R-22 and R-407C although the mass flux of R-404A were higher than other tested refrigerants, because of the most length of evaporator coil fell within the superheated zone.

5. Conclusions

The main findings of the present work are:
1. A simple and detailed evaporator model has been developed for pure and mixture refrigerants R-22, R-134a, R-407C and R-404A.
2. The present model provided detailed information for the evaporator design and performance characteristic. It offers a practical tool for the rating process of an existing water chiller for refrigerant alternatives.
3. The validation of the present evaporator model showed good agreement between experimental and that predicted values.
4. The maximum discrepancy percentage between experimental and predicted evaporator load was (12 %) for all simulated refrigerants. The discrepancy between the measured and the predicted (EWRT) was less than (4 %) for whole operating range.
5. The model showed a good response to the existence of the mass transfer effect on boiling heat transfer coefficient of the zeotropic blends and the overall heat transfer rate.

Nomenclatures

Symbol	Description	Units
A	Area	m^2
Ac	Cross sectional area	m^2
Af	Fin area	m^2
Bo	Boiling number	---
C	Heat capacity	W/K
cp	Specific heat at constant pressure	J/kg.K
Cr	Heat capacity ratio	---
D	Diameter	m
Fr	Froude number	---
G	Mass flux	$kg/m^2.s$
g	Gravitational acceleration	m/s^2
Gr	Grashof number	---
h	Enthalpy	kJ/kg
h_{fg}	Latent heat	J/kg
k	Thermal conductivity	W/m.°C
L	Length of tube	m
M	Molecular weight	kg/kmol
$\dot{m}$	Mass flow rate	kg/s
Nu	Nusselt number	---
p	Pressure	Pa
Pr	Prandtl number	---
Pr	Reduced pressure	---
Q	Heat transfer	W
Re	Reynolds number	---
R_f	Fouling factor	$m^2.°C/W$
R_w	Tube resistance	$m^2.°C/W$
T	Temperature	°C

T_b	Bubble point temperature	°C
T_d	Dew point temperature	°C
T_∞	Surrounding temperature	°C
T_f	Film Temperature	°C
T_{int}	Temperature of liquid vapor interface	°C
T_s	Surface temperature	°C
U	Over all heat transfer coefficient	$W/m^2.°C$
V	Velocity	m/s
We	Weber number	---
X_{tt}	Martinelli parameter	---
X	Vapor quality	---

Greek Symbols:

α	Heat transfer coefficient	$W/m^2.°C$
β	Coefficient of thermal expansion	1/K
ν	Kinematic Viscosity	m^2/s
ΔP	Pressure drop	bar
ε	Effectiveness	---
η	Efficiency	---
η_f	Fin efficiency	---
η_s	Surface efficiency	---
μ	Viscosity	Pa.s
ρ	Density	kg/m^3
σ	Surface tension	N/m
τ	Life time	year

Subscripts:

a	Air
atm	Atmospheric
c	Critical
comb	Combined
evap	Evaporator
frict	Friction
Go	Vapor or Gas only
g	Vapor or Gas
h	Hot
i	Inlet
l	Liquid
Lo	Liquid only
max	Maximum
min	Minimum
nb	Nucleate pool boiling
out	Outlet
r	Refrigerant
sat	Saturated
tp	Two phase
w	Water

Abbreviations:

ASHRAE	American Society of Heating, Refrigerating, and Air-conditioning Engineers, Inc.
ASHTC	Air side heat transfer coefficient
CFC	Chlorofluorocarbon.
EWET	Evaporator water exit temperature
EWFR	Evaporator water flow rate
EWIT	Evaporator water inlet temperature
GWP	Global warming potential
HCFC	Hydro-chlorofluorocarbon.
LFL	Lower flammability limit
LMTD	Logarithmic mean temperature difference

NTU	Number of Transfer Units
ODP	Ozone depletion potential
RLD	Refrigeration load distribution
RSHTC	Refrigerant side heat transfer coefficient

Appendix (A). Typical Experimental Data

Table (A.1). Experimental data for R-22 refrigerant.

Set No. 1		Test Date: 23-3-2009						Refrigerant Type: R-22					Evaporator Water Flow Rate (l/hr): 400					
Test No.	Temperature Measurements					Pressure Measurements					Pressure Drop			Water Side		Air Side		
	T1 (ºC)	T2 (ºC)	T3 (ºC)	T4 (ºC)	T5 (ºC)	P1 (bara)	P2 (bara)	P3 (bara)	P4 (bara)	P5 (bara)	Δp_{evap} (bar)	Δp_{suc} (bar)	Δp_{cond} (bar)	T_{in} (ºC)	T_{out} (ºC)	$T_{d,in}$ (ºC)	$T_{w,in}$ (ºC)	$T_{d,out}$ (ºC)
1	20.00	104	52	11.11	18.33	6.53	21.50	21.43	7.08	6.74	0.34	0.21	0.07	21.11	17.78	26	17	51
2	18.33	102	51	11.11	16.67	6.46	21.22	21.15	7.01	6.74	0.28	0.28	0.07	18.89	15.56	26	17	51
3	16.11	100	49	8.33	13.89	5.98	19.98	19.84	6.60	6.32	0.28	0.34	0.14	16.67	13.33	24	16	46
4	11.11	100	48	7.78	8.33	5.91	19.70	19.57	6.46	6.12	0.34	0.21	0.14	14.44	11.39	24	16	46
5	6.11	96	47	6.11	5.00	5.50	19.08	18.94	6.05	5.70	0.34	0.21	0.14	12.22	9.44	24	16	45
6	5.00	94	47	4.44	3.89	5.29	18.94	18.81	5.84	5.57	0.28	0.28	0.14	10.00	7.78	25	16	45

Table (A.2). Experimental data for R-407C refrigerant.

Set No. 1		Test Date: 24-9-2009						Refrigerant Type: R-407C					Evaporator Water Flow Rate (l/hr): 400					
Test No.	Temperature Measurements					Pressure Measurements					Pressure Drop			Water Side		Air Side		
	T1 (ºC)	T2 (ºC)	T3 (ºC)	T4 (ºC)	T5 (ºC)	P1 (bara)	P2 (bara)	P3 (bara)	P4 (bara)	P5 (bara)	Δp_{evap} (bar)	Δp_{suc} (bar)	Δp_{cond} (bar)	T_{in} (ºC)	T_{out} (ºC)	$T_{d,in}$ (ºC)	$T_{w,in}$ (ºC)	$T_{d,out}$ (ºC)
1	19.44	107	52	11.11	18.33	6.74	21.98	21.84	7.43	7.08	0.34	0.34	0.14	21.11	17.78	26	16	51
2	17.22	107	51.5	10.56	15.56	6.67	21.84	21.70	7.36	7.01	0.34	0.34	0.14	18.89	15.83	25	16	51
3	14.72	107	51	9.44	12.22	6.46	21.29	21.15	7.08	6.74	0.34	0.28	0.14	16.67	13.61	25	15	50
4	8.89	101	48	7.78	8.33	6.12	19.91	19.77	6.74	6.39	0.34	0.28	0.14	14.44	11.67	24	15	47
5	5.56	99	46	6.11	5.00	5.77	19.36	19.22	6.39	6.05	0.34	0.28	0.14	12.22	9.72	24	15	46
6	3.89	97	46	4.44	3.33	5.57	19.22	19.08	6.12	5.77	0.34	0.21	0.14	10.00	7.78	24	15	46

Table (A.3). Experimental data for R-404A refrigerant.

Set No. 1		Test Date: 2-11-2009						Refrigerant Type: R-404A					Evaporator Water Flow Rate (l/hr): 400					
Test No.	Temperature Measurements					Pressure Measurements					Pressure Drop			Water Side		Air Side		
	T1 (ºC)	T2 (ºC)	T3 (ºC)	T4 (ºC)	T5 (ºC)	P1 (bara)	P2 (bara)	P3 (bara)	P4 (bara)	P5 (bara)	Δp_{evap} (bar)	Δp_{suc} (bar)	Δp_{cond} (bar)	T_{in} (ºC)	T_{out} (ºC)	$T_{d,in}$ (ºC)	$T_{w,in}$ (ºC)	$T_{d,out}$ (ºC)
1	13.33	90	45	12.22	13.33	6.60	20.74	20.60	7.29	7.01	0.28	0.41	0.14	21.11	17.78	24	16	51
2	11.11	87	43	10.56	11.11	6.26	19.77	19.63	6.94	6.60	0.34	0.34	0.14	18.89	15.56	24	16	49
3	9.44	83	41	8.89	9.44	5.91	18.94	18.81	6.60	6.26	0.34	0.34	0.14	16.67	13.61	23	16	48
4	7.78	79	40	7.22	7.78	5.63	18.53	18.39	6.26	5.98	0.28	0.34	0.14	14.44	11.94	23	16	46
5	6.11	77	39	5.56	6.11	5.43	18.26	18.12	5.98	5.70	0.28	0.28	0.14	12.22	9.44	23	16	46
6	5.00	75	38	4.44	5.00	5.15	17.70	17.57	5.70	5.43	0.28	0.28	0.14	10.00	7.78	23	16	45

Table (A.4). Experimental data for R-134a refrigerant.

Set No. 2		Test Date: 16-7-2009						Refrigerant Type: R-134a					Evaporator Water Flow Rate (l/hr): 400					
Test No.	Temperature Measurements					Pressure Measurements					Pressure Drop			Water Side		Air Side		
	T1 (ºC)	T2 (ºC)	T3 (ºC)	T4 (ºC)	T5 (ºC)	P1 (bara)	P2 (bara)	P3 (bara)	P4 (bara)	P5 (bara)	Δp_{evap} (bar)	Δp_{suc} (bar)	Δp_{cond} (bar)	T_{in} (ºC)	T_{out} (ºC)	$T_{d,in}$ (ºC)	$T_{w,in}$ (ºC)	$T_{d,out}$ (ºC)
1	20.6	88	45	12.2	18.6	4.26	13.7	13.57	4.94	4.6	0.34	0.34	0.14	20.28	18.06	29	20	49
2	18.9	90	45	12.2	16.1	4.32	13.7	13.57	4.94	4.6	0.34	0.28	0.14	18.61	16.39	28	20	49
3	10	89	44.5	11.7	10	4.26	13.57	13.43	4.91	4.53	0.38	0.28	0.14	17.22	15	28	20	48.5
4	8.3	84	44	10.6	8.9	4.05	13.29	13.15	4.74	4.32	0.41	0.28	0.14	15.83	13.89	28	20	48
5	7.8	77	43	10.3	7.8	3.98	13.15	13.01	4.67	4.26	0.41	0.28	0.14	15.00	13.33	27	20	47.5
6	7.2	73	42.5	9.4	7.2	3.91	12.94	12.81	4.6	4.19	0.41	0.28	0.14	13.89	12.22	27	20	47
7	6.1	69	42	8.9	6.1	3.77	12.88	12.74	4.46	4.05	0.41	0.28	0.14	12.78	11.11	27	20	46

References

[1] Patil, R. K., Shende, B.W. and Ghosh, P.K., "Designing a Helical coil Heat Exchanger", Chemical Engineering Journal, pp.85-88, December (1982).

[2] Domanski, P. A., "EVSIM - an Evaporator Simulation Model Accounting for Refrigerant and One Dimensional Air Distribution", NISTIR 89-4133, U.S. Dept. of Commerce, NIST, Maryland 20899, (1989).

[3] Vina, J. M., "The Modeling of a Natural Convection Heat Exchanger in a solar Domestic Hot Water System", M.Sc. Thesis, University of Wisconsin-Madison, College of Engineering, (1994).

[4]   Naphon, P., "Thermal performance and pressure drop of the helical-coil heat exchangers with and without helically crimped fins", Int. Communication of Heat Mass Tran, Vol.34 (3), pp.321–330, (2007).

[5]   Amitkumar, S. P., and Andhare, A.M., "Design and Thermal Evaluation of Shell and Helical Coil Heat Exchanger", International Journal of Research in Engineering and Technology (IJRET), Vol. 04 Issue: 01, pp.416-423, January (2015), Available @ http://www.ijret.org

[6]   Mahmood, D. M., "Experimental and Theoretical Evaluation for the Evolution in Alternatives Applications in Water Chillers", MSc. Thesis, Mechanical Engineering Department, College of Engineering, Al-Mustansiriya University, Baghdad, Iraq, (2010).

[7]   ASHRAE Handbook, "HVAC systems & Equipment", American Society of Heating, Refrigeration, and Air Conditioning Engineers, Inc., New York, (1979).

[8]   Tarrad, A. H. and Mohammed, A. G.," A Mathematical Model for Thermal-Hydraulic Design of Shell and Tube Heat Exchanger Using a Step by Step Technique", Engineering and Development Journal, Vol. 10, No. 4, pp. 12-35, December (2006).

[9]   Tarrad, A. H.," A Numerical Model for Thermal-Hydraulic Design of a Shell and Single Pass Low Finned Tube Bundle Heat Exchanger", Engineering and Technology Journal, Vol. 25, No. 4, pp. 619-645, (2007).

[10] Tarrad, A. H., "A Numerical Model for Performance Prediction of Dry Cooling Conditions of Air Cooled Condensers in Thermal Power Plant Stations", Engineering and Technology Journal, Vol. 28, No. 16, pp. 5271-5292, (2010).

[11] Tarrad, A. H. and Al-Nadawi, A. K., "Modeling of Finned-Tube Evaporator using Pure and Zeotropic Blend Refrigerants", ATINER Conference Paper Series No: TEN2015-1548, Athens, (2015).

[12] Tarrad, A. H., "A Numerical Analysis of Adiabatic Capillary Tube Performance in Vapor Compression Refrigeration Systems", The Iraqi Journal for Mechanical and Materials Engineering, Vol. 8, No. 3, pp. 201-218, (2008).

[13] Incropera, F. P. and DeWitt, D. P., "Fundamentals of Heat and Mass Transfer", Fourth Edition, John Wiley & Sons, New York, (1996).

[14] Gungor, K.E. and Winterton, R.H.S., "A General Correlation for Flow Boiling in Tubes and Annuli", Int. Journal of Heat and Mass Transfer, Vol. 29, No.3, pp. 351-358, (1986).

[15] Chen, J.C., "A Correlation for Boiling Heat Transfer to Saturated Fluids in Convective Flow, Ind. Eng. Chem. Proc. Des. Dev., 5, pp. 322-329, (1966).

[16] Cooper, M.G., "Saturation Nucleate Pool Boiling, A Simple Correlation," 1st U.K. National Conference on Heat Transfer, Vol. 2, pp. 785–793, (1984).

[17] Gungor, K.E. and Winterton, R.H.S., "Simplified General Correlation for Saturated Flow Boiling and Comparisons of Correlations with Data", Chem. Eng. Res. Des., Vol. 65, pp 148-156, (1987).

[18] Thome, J. R., "Boiling of New Refrigernts: A State-of-the-Art Review", Int. J. Refrig., Vol. 19, No. 7, pp. 435-457, (1997).

[19] Bivens, D.B., and Yokozeki, A., "Heat Transfer Coefficients and Transport Properties For Alternative Refrigerants", Proc. International Refrigeration Conference at Purdue, Purdue University, West Lafayette, Indiana, USA, July (1994).

[20] Cengel, Y. A., "Heat Transfer", International Edition, MC. Graw-Hill Book Company, (1998).

[21] Churchill, S.W. and Chu, H.H.S., "Correlating Equations for Laminar and Turbulent Free Convection from a Horizontal Cylinder", International Journal of Heat and Mass Transfer, Vol. 18, pp.1049-1053, (1975).

[22] Holman, J. P., "Heat Transfer", Ninth Edition, McGraw-Hill Book Company, (2002).

[23] McQuiston, F. C. and Parker, J. P., "Heating, Ventilating and Air-Conditioning Analysis and Design", John Wiley & Sons, (1994).

[24] Tarrad, A. H., "Pool Boiling of Pure Fluids and Mixtures on Plain and Enhanced Surfaces", Ph.D. Thesis, Mech. Eng., Heriot-Watt University, Edinburgh, U.K., (1991).